

Chemical Looping Combustion: One Answer to Sequestering Carbon Dioxide

J.S. Dennis*

University of Cambridge, Department of Chemical Engineering and Biotechnology, Pembroke Street, Cambridge, CB2 3RA, England.

Abstract

Chemical-looping combustion (CLC) has the inherent property of separating CO₂ from flue gases. Instead of air, it uses an oxygen-carrier, usually in the form of a metal oxide, to provide oxygen for combustion. This paper reviews the application of chemical looping to the combustion of *solid* fossil fuels. There is little doubt that chemical looping combustion for the combustion of *gaseous* fuels could be brought to the industrial scale readily; however, further research on the important topic of solid fuels is needed. In principle, there are three options for coping with solid fuels. (i) The solid fuel is gasified separately and the synthesis gas burnt in a conventional chemical looping arrangement for gaseous fuels. (ii) The solid fuel is gasified *in situ* in the presence of a batch of metal oxide in a single reactor. As the metal oxide becomes depleted, the feed of fuel is discontinued, the inventory of fuel is reduced by further gasification and then the contents are re-oxidised by the admission of air to the reactor. (iii) The solid fuel is gasified *in situ* in the presence of the metal oxide, as in (ii), but the unburnt fuel is separated from the spent oxide, with the latter being recycled through an oxidation reactor. In each case, the gasifying agent would need to be free from nitrogen, *e.g.* a mixture containing CO₂ and steam only. The advantages and disadvantages of each are discussed, and some research on option (ii) at Cambridge is surveyed. This paper also examines a modification of chemical looping, involving the oxides of iron in packed bed reactors, to produce hydrogen of high purity from low-grade synthesis gas. This offers substantial benefits and, indeed, might be a low cost option for the initial industrial realisation of the looping technique. It is concluded that the chemical looping of solid fuels has been demonstrated to be feasible at the small scale and that it is timely for there to be a major European initiative to work on the scale-up and industrial demonstration of the technique.

1. INTRODUCTION

The urgent need to apply chemical looping techniques to solid fuels stems from the requirement to capture and sequester the CO₂ emitted from the expanding use of coal for the generation of electricity [1-6]. The global supply of electricity accounts for ~38% of total anthropogenic carbon emissions to the atmosphere or ~2,400 Mte/y (carbon basis), a figure projected to exceed 4,000 Mte/y by 2020 [5]. The principal means of controlling emissions from the use of coal of fossil-derived CO₂ will be to capture it from flue gases and sequester it in suitable geological structures. Such disposal is only feasible if the CO₂ is available in almost pure form, largely free of nitrogen and other gases [7]. To capture CO₂ from the current generation of coal-fired power plants, many of which use pulverised fuel (pf) firing, the commercial focus is, rightly, on adapting commercial, or near-commercial, technology, such as [8] (i) scrubbing the flue gases from the combustion of coal in air with amines to remove CO₂, (ii) pulverised fuel firing with oxyfuel, or integrated gasification combined cycle with pre-combustion capture of CO₂. These all impose significant efficiency and capital cost penalties [8].

2. BASIS OF CHEMICAL LOOPING

Chemical looping combustion (CLC) offers the inherent feature of isolating CO₂, avoiding the need for costly separation processes. The basic concept for the

combustion of *gaseous* fuels involves two interconnected fluidised beds; the fuel enters the *fuel reactor*, which contains a metal oxide, MeO, and reacts: $(2n + m) \text{MeO} + \text{C}_n\text{H}_{2m} \rightarrow (2n + m) \text{Me} + m\text{H}_2\text{O} + n\text{CO}_2$ (a), so that the exit stream contains largely CO₂ and steam, yielding almost pure CO₂ when the steam is condensed. The reduced metal oxide, Me, is transferred to the *oxidation reactor*, where it is oxidised: $\text{Me} + 1/2\text{O}_2 \rightarrow \text{MeO}$ (b). The oxidised MeO is recycled to the first reactor to begin a new cycle of reduction and oxidation and thus acts as an *oxygen carrier*. A full conversion from MeO to Me and *vice versa* is not necessarily obtained in a real system, neither is it essential [7,9]. The exit gas from the oxidation reactor is N₂ containing unused O₂. Taking reactions (a) and (b) together, the fuel has been combusted but the resulting CO₂ has been separated from the N₂ in the air, whilst the total heat evolved is the same as for the combustion of the fuel in air. Depending on the metal oxide, reaction (a) is often, but not always, endothermic; reaction (b) is always exothermic. When the two reactors are fluidised beds, and where reaction (a) is endothermic, it is possible to use the interchange of the solid oxygen carrier between the beds to balance the heat on the fuel reactor. The heated, depleted air leaves the oxidation reactor at high temperature (*ca.* 1000°C) and can be used to raise steam, or, when the operation is pressurised, to drive a gas turbine topping cycle. This technique for the combustion of gaseous fuels, particularly natural gas, has been an active research area for the last two decades, with work on oxygen carriers [10-13], reactor design [7,9,14,15,21] and

* Corresponding author: jsd3@cam.ac.uk
Proceedings of the European Combustion Meeting 2009

thermodynamic efficiency [16-20]. There have been significant advances towards industrial demonstration with gaseous fuels, with the groups at Chalmers University, Sweden, and at the Instituto de Carboquímica (CSIC/ICB), Spain being in the van of these developments [14,21].

Process Thermodynamics

There have been numerous studies on efficiency [16-20]. Kvamsdal *et al.* [18] studied nine concepts for natural-gas fired power plants, using a 400 MW combined cycle without CO₂ capture as a basis for comparison. On the basis of net efficiency (% LHV), the base case had an efficiency of 57%. The use of CLC for CO₂ capture gave a reduction to 51%, oxyfuel to 47% and amine scrubbing of the flue gas, with air as

occurs owing to the irreversibility of heat transfer from 2222 K to 1273 K, given by $T_0 \Delta H_T^0 \left[\frac{1}{T} - \frac{1}{T_a} \right] = 81.5$

kJ/mol. Thus, the loss in the ideal work is $[(81.5 + 106.6)/801.0] \times 100\% = 23.5\%$. Consider, now, the combustion occurring *via* the looping reactions (2) (reduction) and (3) oxidation. In this case, $-T_0 \Delta G_T^0 / T$

can be applied to each reaction in turn, where $T = 673$ K is about the minimum at which the reduction would feasibly occur and 1273 K the upper limit that the solid oxide could withstand without significant sintering and degradation in performance. This gives an overall loss in the theoretically available work of 115.5 kJ/mol. There is no loss in transfer to the turbine inlet

Table 1. Thermodynamics of Selected Reactions. Calculated from McBride *et al.* [22]

Reaction	Temp., T K	ΔH_T^0 kJ/mol	ΔG_T^0 kJ/mol	ΔH_{298K}^0 kJ/mol	ΔG_{298K}^0 kJ/mol
1 CH ₄ (g) + 2O ₂ (g) → CO ₂ (g) + 2H ₂ O(g)	2222	-814.9	-794.2	-802.6	-801.0
2 4.505Fe ₂ O ₃ (s) + CH ₄ (g) → 9.514Fe _{0.947} O(s) + CO ₂ (g) + 2H ₂ O(g)	673	370.6	-4.6	377.1	210.7
3 9.514Fe _{0.947} O(s) + 2O ₂ (g) → 4.505Fe ₂ O ₃ (s)	1273	-1121.3	-493.1	-1179.7	-1011.7
4 4CuO(s) + CH ₄ (g) → 4Cu(s) + CO ₂ (g) + 2H ₂ O(g)	1173	-208.1	-593.9	-180.0	-289.4
5 4CuO(s) + CH ₄ (g) → 4Cu(s) + CO ₂ (g) + 2H ₂ O(g)	623	-186.6	-406.8	-180.0	-289.4
6 4Cu(s) + 2O ₂ (g) → 4CuO(s)	1173	-594.5	-206.4	-622.6	-511.6

oxidant, 48%. These performances for no abatement, oxyfuel and amine scrubbing compare favourably with the study of Davison [8] giving 55.6%, ~45% and 48%, respectively, suggesting that the value [18] for CLC is reasonable. Of course, CLC is strictly an emerging technology and so subject to uncertainty, but these figures suggest that it deserves serious consideration.

The original interest in CLC, *e.g.* [16,20], was motivated by its potential to reduce the thermodynamic irreversibility of combustion. The ideal, reversible work obtainable from the combustion of methane (Table 1, reaction (1)), ignoring the small adjustment for the entropy of mixing and assuming that the reactants and products are at the environmental temperature, $T_0 = 298.15$ K, and pressure, is equal to the exergy change = $-\left[\Delta H_{298K}^0 - T_0 \Delta S_{298K}^0 \right] = -\Delta G_{298K}^0 = 801.0$ kJ/mol. Combustion processes are far from being reversible: the lost work in a such a reaction occurring irreversibly at temperature, T , is [23] equal to $-T_0 \Delta G_T^0 / T$. Since the adiabatic flame temperature for the combustion of methane in air is ~2222 K, the lost work in the reaction itself is $(-298.15 \times -794.2/2222) = 106.6$ kJ/mol. If the maximum working temperature for a device using the combustion, *e.g.* a turbine, is $T_a = 1273$ K, a further loss

temperature (1273 K) in this case, so the theoretical loss of available work has been reduced to $[115.5/801.0] \times 100\% = 14.4\%$, a net improvement. Some looping materials, *e.g.* Cu and its oxides, are exothermic in both oxidation and reduction, in which case the highest possible temperatures in both oxidation (reaction (6) at 1173 K) and reduction (reaction (4)) are required: the lost work would be ~25%, compared to 31% with reaction (5) at the lowest temperature at which CuO can be reduced.

3. CLC OF SOLID FUELS

Techniques

In contrast to the use of CLC with *gaseous* fuels, only limited research has been published [2-4, 24-27] on CLC with solid fuels, mainly because the particles of fuel and oxygen-carrier cannot be easily separated. Without separation, the solid fuel would enter the oxidation reactor along with the recycling oxygen carrier and give CO₂ in the off-gas, thereby defeating the object of the technique. To circumvent this, three broad strategies have evolved:

(i) *Gasify the solid fuel separately and burn the synthesis gas using a conventional chemical looping arrangement for gaseous fuels* [28-30]. Better combustion efficiencies, with reduced coking, are

obtained with synthesis gas as opposed to natural gas, e.g. [2,28,31]. However, there is a significant problem. The gasifying agent would need to be pure O₂, or a mixture of O₂ and CO₂, to ensure that the synthesis gas were mainly CO and H₂, without N₂. This would require an air separation unit and defeat the object of using the chemical looping technique. Alternatively, the gasification could be undertaken in pure CO₂ or mixtures of CO₂ and steam, but to balance these endothermic gasification reactions, heat would have to be transferred to the gasifier from the oxidation reactor. This is not impossible, but it does complicate reactor design. One possibility is to use the packed bed configuration, described later in this article, or to design a concentric fluid bed arrangement whereby heat transfer can take place from the air reactor to the gasifier, both fluidised, *via* a shared vessel wall.

(ii) *Gasification in situ in a Cyclic Batch Operation.* A criticism of the basic CLC technique is the conveying of large quantities of solids between reactors and the concomitant problems of attrition, wear and dust. However, extended pilot trials are now suggesting that attrition of solids can be kept within reasonable bounds [14,27]. Accordingly, another technique [3,26] involves the *in situ* gasification and combustion of solid fuel using one fluidised bed. This reactor operates in a cycle of three consecutive periods: t_1 , t_2 and t_3 . During t_1 , solid fuel is fed continuously to a bed of oxygen-carrier, fluidised by steam or CO₂, or both. Firstly, the fuel loses its volatile matter, which is oxidised by the oxygen-carrier. Next, the fluidising gas gasifies the resulting char, producing synthesis gas, which immediately reacts with the oxygen-carrier to form CO₂ and steam. At the end of t_1 , the feed of coal is stopped and the remaining inventory of carbon is allowed to gasify and combust for a further period, t_2 , until the inventory of char is sufficiently small. At the end of t_2 , the bed is fluidised by air instead of steam or CO₂ for a period of time, t_3 , when the depleted oxygen-carrier is regenerated. A new cycle then starts. In practice, several reactors would be used, operating at various phases in the cycle to even the load to the downstream power cycle. Indeed, where the solid fuel gives a very reactive char (e.g. biomass), it might be that the second phase is omitted since the inventory of fixed carbon in the bed would be low. Much remains to be worked out at the pilot scale, however. This scheme is contingent on the reduction of the oxygen-carrier being sufficiently exothermic to balance the endothermic gasification reactions during t_1 and t_2 . Thus, the choice of oxide is narrowed significantly. In our work [31], the focus has been to produce a Cu-based oxygen-carrier for CLC. CuO was chosen because it is cheap, is of relatively low toxicity and is good at transferring oxygen. Most importantly, its exothermic reduction reaction can provide heat for the endothermic gasification of a solid fuel to form synthesis gas, which is subsequently burned by contacting the CuO. The relevant reducing and oxidation reactions of the oxygen-carrier are discussed later in this paper.

(iii) *Gasify the solid fuel in situ in the presence of the metal oxide in pure CO₂ or steam or mixtures thereof: separate the unburnt fuel from the spent oxide before the solids are passed to the oxidation reactor.* Lyngfelt and colleagues [4,27] have developed a fuel reactor designed to separate the unburnt fuel from the spent metal oxide before the carrier is recycled to the air reactor. The overall plant consists of an air reactor, operated as a fast fluidised bed, connected to a riser leading to a cyclone, where elutriated particles are separated. This section is similar to that used previously in work on natural gas combustion [14]. The fuel reactor, however, has been modified so that (a) gasification and reaction occurs, and (b) the solids pass to a downstream section where a separation can be effected between the fuel particles and the carrier (ilmenite, FeTiO₃, mean size 150 µm) on the basis of different elutriability of the carrier and the fuel particles, the latter being of lower density and, most likely, smaller in size at this stage. Initial results [27] are impressive: the system was tested for 22 h at temperatures above 850°C, using natural ilmenite as the carrier and a South African coal as the solid fuel. The overall capture of CO₂ ranged from 82 to 96% of the incoming fuel.

Choice of Carrier

There is a voluminous literature on the choice of metal carriers and recent reviews have been undertaken, *inter al.*, by Anthony [1] and Hosain & de Lasa [32]. The metal oxide of interest has usually been supported on an inert matrix to provide resistance against mechanical, chemical and thermal stresses over the many cycles of operation required. Such supporting solids also ensure that the metal oxide is well-dispersed, thereby minimising thermal sintering and agglomeration of the metal oxide particles. For example, de Diego *et al.* [12] found that when tested in a thermogravimetric analyser, unsupported CuO lost 90% of its initial reactivity within 3 cycles of operation. However, CuO supported on SiO₂ maintained its initial reactivity over many cycles. Various authors [12,31,34-36] have shown that CuO, when mixed with Al₂O₃, displays a high conversion to metallic Cu over many cycles. The reactivity of the four, most-studied, supported oxygen-carriers is in the descending order of NiO > CuO > Fe₂O₃ > Mn₂O₃ [35,37-40]. The Ni-based carrier in its reduced state has the undesirable property of catalysing the formation of carbon when methane is the fuel [34,38]; there are also concerns about the toxicity of nickel compounds. Apart from oxides of transition metals, CaSO₄ has also received attention as an oxygen carrier, cycling between CaS and CaSO₄ [1,2,33]. The main reason for this is that there are large amounts of natural gypsum available worldwide and also that CaSO₄ has a high oxygen carrying capacity, compared to metal oxides. A serious side reaction is reduction to CaO and the release of H₂S when synthesis gas is used, and, during the reoxidation, the oxidation of CaS to CaO and SO₂, rather than CaSO₄. The release of sulphurous species is a problem: e.g. in Song *et al.*'s

experiments [2] using synthesis gas, up to 5000 ppm SO₂ and 2000 ppm H₂S in the off-gases were variously detected. The steady conversion to CaO, and the reduction in reactivity of the CaS after ~20 cycles of operation, is also problematic. For use with solid fuels, a number of considerations affect the choice of oxide and whether or not it is supported:

- (i) thermodynamics and chemical reactivity,
- (ii) the susceptibility of the carrier particles to attrition and fragmentation, resulting in loss from the system,
- (iii) oxygen carrying capacity, *viz.* the mass of oxygen supplied per unit mass of carrier in its oxidised state,
- (iv) the susceptibility of the carrier particles to the effects of contaminants, *e.g.* the effect of sulphur in the fuel or the tendency to form fusible compounds with the ash, particularly under reducing conditions,
- (v) the loss of reactivity after many cycles, caused, for example, by sintering effects, and
- (vi) for fluidised systems, the typical density and size of particles needed: particles of significant density and size will present problems with the design of fast fluidised beds and with the erosion of equipment.

Cost is important; given the number of potential mechanisms for deactivation or loss of carrier, it might be better to use cheap materials even though they might not have the same longevity as materials of higher cost.

Thermodynamic Considerations

(i) *Enthalpy of Reaction.* For the cyclic batch case, considered above, suppose that the solid fuel is a pure carbon so that the gasification reaction in the oxide-reducing phase is:



This reaction is balanced, when CuO is used, by reaction (8) followed by reaction (9), in Table 2, of -98 kJ/mol. When iron is used, reaction (7) is followed by reaction (15) in Table 2, giving a net enthalpy of +92 kJ/mol and so being a net heat sink. During the oxidation phase, the net enthalpy produced by Cu and Fe₃O₄ is, respectively, -297.3 (reactions (12) and (13)) and -486.6 (reaction (19)) kJ/mol O₂ used. Thus, without an enthalpy coupling in the case of iron oxide, it would not be possible to use the looping scheme proposed here, whereas with a copper looping agent, the reaction is always exothermic without coupling. Thus, for the arrangement used by Lyngfelt [14], which used natural ilmenite, the enthalpy balance is maintained by the circulation of solids from the oxidation reactor. Leion *et al.* [4] conducted experiments on the *in situ* gasification of petroleum coke with CO₂ in the presence of an iron-based carrier. Assuming that the heat requirement of the fuel reactor was 0.2 MW and the heat released in the oxidation reactor was 1.2 MW for an assumed overall output of 1 MW, they estimated that the solids circulation rate needed would be about 6.3

kg/s to balance the sensible heat needed to heat the incoming CO₂ to the reactor temperature (0.084 MW) and to supply the heat of reaction (0.2 MW). They concluded that the total inventory of carrier (60 wt % Fe₂O₃) would be less than 2000 kg/MW thermal output for this system.

(ii) *Feasibility of Reaction.* Using values of $\Delta G_{1173\text{K}}^0$ from Table 2 to evaluate relevant equilibrium constants, it can be shown that at an operating temperature of 900°C, the reduction of CuO would be complete provided the ratio of partial pressures of CO to CO₂ present, $P_{\text{CO}}/P_{\text{CO}_2}$, exceeds $\sim 4.6 \times 10^{-5}$. In practice, of course, this would be the case and so, thermodynamically, there should be complete reduction of CuO in the fuel reactor. Copper metal would be fully oxidized to CuO at an operating temperature of 1173 K, provided the partial pressure of oxygen, P_{O_2} , exceeds ~ 0.02 bar. Since the proposed oxidant is air, which has a mole fraction of oxygen of 0.21, the oxidation would indeed go to completion in a correctly-designed oxidation step. Calculations also show that for the reduction of Fe₂O₃ to Fe_{0.947}O or Fe at 900°C (1173K), $P_{\text{CO}}/P_{\text{CO}_2}$ must exceed 0.6 and 3.1, respectively. These figures are much higher than the corresponding ratio needed for the reduction of Fe₂O₃ to Fe₃O₄ (1.5×10^{-5}), indicating that only the reduction to Fe₃O₄ is likely to be possible in combusting systems. Calculations for the oxidation of Fe indicate that, at, *e.g.* 900°C, a partial pressure of oxygen exceeding 3.6×10^{-7} bar is required to oxidise it to Fe₂O₃. This is much lower than the likely partial pressure during the oxidation phase with air and so, thermodynamically, would proceed to completion.

4. SOME RESEARCH AT CAMBRIDGE ON LOOPING COMBUSTION USING CYCLIC BATCH PROCESSES

Initial Illustration

To illustrate the basic technique, our initial feasibility studies [2,26] concentrated on iron oxide as the oxygen carrier, since it is relatively easy to prepare and does not agglomerate or sinter at the projected operating temperatures. As will be seen later, this is also true of CuO, but the preparation of this as a robust carrier has taken some considerable research [31].

Materials. The chemical looping agent was produced from Fe₂O₃ powder (> 99% purity), which was mixed with a small amount of distilled water, in a mechanical mixer. The resulting particles were sieved to +300, -710 μm, and any larger lumps broken up. The procedure was repeated until a sufficient quantity of particles was in this size range. The agglomerated particles of Fe₂O₃ were then placed in a furnace, heated to 900 °C and maintained at this temperature for 5 h. The resulting particles were then sieved into defined size ranges, *e.g.* 425 to 710 μm.

Apparatus and Experimental Technique. Initial experiments to test the feasibility of chemical looping were performed in a small fluidised bed of either (i) 20

ml of silica sand (+355,-425 μm) or (ii) ~ 10 g of Fe_2O_3 (+300,-425 μm) made up to 20 ml with silica sand. These particles were contained in a quartz tube (i.d. 30 mm) with a sintered disk for a distributor. It was fluidised by N_2 (85 ml s^{-1} at STP) mixed with either pure CO_2 (32 ml s^{-1} at STP) for gasification, or air (28 ml s^{-1} at STP) to regenerate the Fe_2O_3 . U/U_{mf} was between 9 and 12. The reactor was placed in a tubular furnace and the bed was heated to 900°C . The off-gases were sampled continuously into two NDIR analysers,

completion in every experiment. The experiment was repeated several times. The second set of experiments used the bed containing the particles of Fe_2O_3 mixed with silica sand. As in the first experiments, a batch of char (~ 0.1 g) was added to the bed and gasified to completion. Further batches of char were added, until it was clear that the chemical looping agent (Fe_2O_3) had been used up. At this point, the bed was re-oxidised with the mixture of air and N_2 ; then the gasification experiment was repeated. Further gasification

Table 2. Thermodynamic Information for Selected Reactions with Synthesis Gases. [22]

	Reaction	ΔH_{1173K}^0 kJ/mol	ΔG_{1173K}^0 kJ/mol
8	$2\text{CuO(s)} + \text{CO(g)} \rightarrow \text{Cu}_2\text{O(s)} + \text{CO}_2\text{(g)}$	-151.4	-160.6
9	$\text{Cu}_2\text{O(s)} + \text{CO(g)} \rightarrow 2\text{Cu(s)} + \text{CO}_2\text{(g)}$	-115.2	-97.4
10	$2\text{CuO(s)} + \text{H}_2\text{(g)} \rightarrow \text{Cu}_2\text{O(s)} + \text{H}_2\text{O(g)}$	-118.4	-162.9
11	$\text{Cu}_2\text{O(s)} + \text{H}_2\text{(g)} \rightarrow 2\text{Cu(s)} + \text{H}_2\text{O(g)}$	-82.1	-99.7
12	$2\text{Cu(s)} + 0.5\text{O}_2\text{(g)} \rightarrow \text{Cu}_2\text{O(s)}$	-166.8	-83.2
13	$\text{Cu}_2\text{O(s)} + 0.5\text{O}_2\text{(g)} \rightarrow 2\text{CuO(s)}$	-130.5	-20.0
14	$\text{CO(g)} + \text{H}_2\text{O(g)} \rightarrow \text{CO}_2\text{(g)} + \text{H}_2\text{(g)}$	-33.1	+2.4
15	$3\text{Fe}_2\text{O}_3\text{(s)} + \text{CO(g)} \rightarrow 2\text{Fe}_3\text{O}_4\text{(s)} + \text{CO}_2\text{(g)}$	-38.6	-108.2
16	$0.947\text{Fe}_3\text{O}_4\text{(s)} + 0.788\text{CO(g)} \rightarrow 3\text{Fe}_{0.947}\text{O(s)} + 0.788\text{CO}_2\text{(g)}$	+16.7	-5.5
17	$3\text{Fe}_2\text{O}_3\text{(s)} + \text{H}_2\text{(g)} \rightarrow 2\text{Fe}_3\text{O}_4\text{(s)} + \text{H}_2\text{O(g)}$	-5.5	-110.6
18	$0.947\text{Fe}_3\text{O}_4\text{(s)} + 0.788\text{H}_2\text{(g)} \rightarrow 3\text{Fe}_{0.947}\text{O(s)} + 0.788\text{H}_2\text{O(g)}$	+42.8	-7.3
19	$2\text{Fe}_3\text{O}_4\text{(s)} + 0.5\text{O}_2\text{(g)} \rightarrow 3\text{Fe}_2\text{O}_3\text{(s)}$	-243.3	-72.4

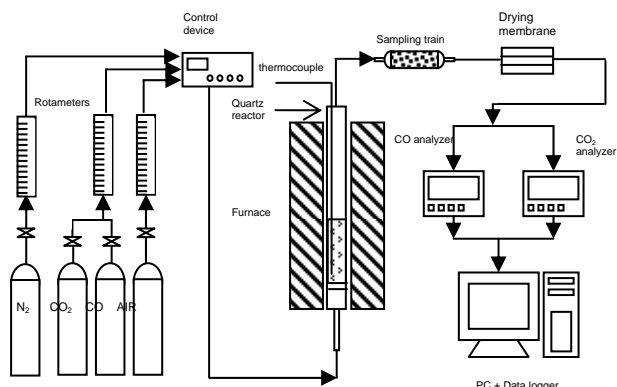


Fig. 1. Experimental arrangement.

one measuring $[\text{CO}_2]$ and $[\text{CO}]$ (with ranges of 20 mol% and 1 mol%, respectively) and the other $[\text{CH}_4]$ and $[\text{CO}]$ (with ranges of 6 mol% and 11 mol%, respectively), *via* a trap at 0°C (to remove tars *etc.*) with a filter and a membrane drier, shown in Fig. 1.

The first experiments used the bed of silica sand alone and served as a control. With the hot bed fluidised by the mixture of N_2 and CO_2 , a batch (~ 0.1 g) of a char (85 wt% C, 0.71 wt% H, 0.7 wt% N, 12 wt% ash, balance O) made from Hambach lignite was added to the bed. The char was allowed to gasify until

experiments were repeated with the parent coal (sieved to 1.4 to 1.7 mm) added, instead of its char.

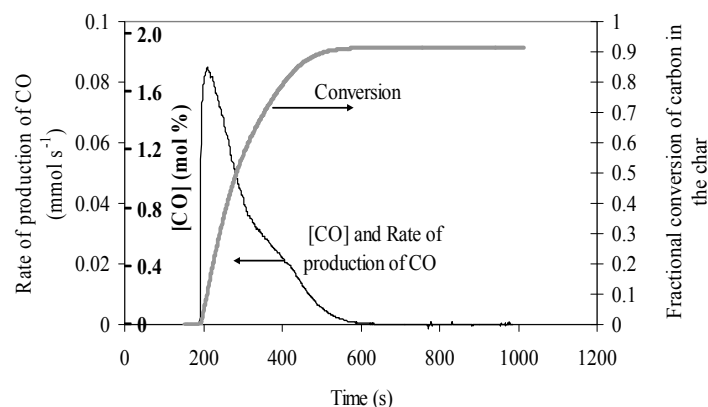


Fig. 2. The rate of production of CO from a bed of sand (i.e. the product of the total molar flow rate and mole fraction of CO) in which a single batch of char (0.0904g) was gasified in 27.5 mol% CO_2 at 900°C .

Results. A typical result, *without* looping agent present, is shown in Fig. 2 indicating that gasification of the char was complete within ~ 500 s. The peak rate of gasification in Fig. 2 corresponded to a mole fraction of

1.8 mol% of CO in the off-gas from the bed. The conversion of the carbon in the char to CO, as measured from the area under the curve in Fig. 2, was between 90.0% and 91.7% in 4 replicated experiments. Since a small amount of fine carbon was collected by the trap in the sampling line, the discrepancy of ~10 % in the mass balance can be partly attributed to the elutriation of fine particles of char, once most of a batch had been gasified.

Figure 3 shows the results of experiments in which a batch of char was gasified in CO₂, in a bed initially of sand and Fe₂O₃ particles. In this case reaction (7) again produces CO, which is subsequently oxidised in reaction (15) (Table 2) by the solid particles of Fe₂O₃. The recovery is here defined as the number of moles of CO actually produced in the off-gases to the amount which would have been produced had all the carbon in the char been gasified to CO. The bed was not regenerated between the first four experiments; consequently, the ability of the Fe₂O₃ particles to react with CO was gradually reduced. The largest peak concentration in Fig. 3 corresponds to ~2 mol%; it occurs when the Fe₂O₃ was fully reduced and exhausted. This is evident from the fact that the maximum [CO] agrees well with the 1.8 mol% observed with a bed of sand, in Fig. 2. The very last plot for CO in Fig. 3 is identical to the first, showing that all the Fe₂O₃ had been regenerated after being exposed to 5 mol% O₂ for ~ 5 min. Subsequent experiments with the parent coal [2], not shown, indicate that the volatiles also react with Fe₂O₃ and do so rapidly. Our work also suggests that

there is an improved conversion of volatile matter, including its tarry components. Of course, it is possible that the volatile matter, before it is oxidised by the Fe₂O₃, is also cracked by it. These experiments demonstrate that it is possible to use a solid fuel, such as coal, directly within a chemical looping cycle, involving gasification of the char as well as combustion of both the volatiles and the products of gasification by reaction with Fe₂O₃. If it is assumed that the Fe₂O₃ in the bed reacts to form Fe₃O₄ in reactions (7) and (15), so that the overall reaction in the system is:



the theoretical capacity of a bed (containing 10.308 g of Fe₂O₃, as used to generate the results in Fig. 3) is 0.0106 mol of carbon. The assumption that the Fe₂O₃ reacts to form only Fe₃O₄ (rather than Fe_{0.947}O or metallic Fe) can be justified by the following thermodynamic argument. For reaction (16) from Table 2, in which Fe₃O₄ is reduced to Fe_{0.947}O, the equilibrium constant $K_p = (P_{CO_2}/P_{CO})^{0.788} = 1.75$ at 900°C. Thus, at 900 °C, for the Fe₃O₄ to be reduced to Fe_{0.947}O would require $P_{CO}/P_{CO_2} > 0.49$, which it was not. A rough estimate of the actual capacity of the bed can be calculated by noting that in Fig. 3, the Fe₂O₃ had been depleted after the third batch had been added. Using the difference in yields of CO between the inert bed of sand and the active bed containing Fe₂O₃, the amount of carbon consumed by reaction (20) was 0.0117 mol, in close agreement with the above theoretical value of 0.0106 mol. This simple calculation indicates that the Fe₂O₃ goes completely to

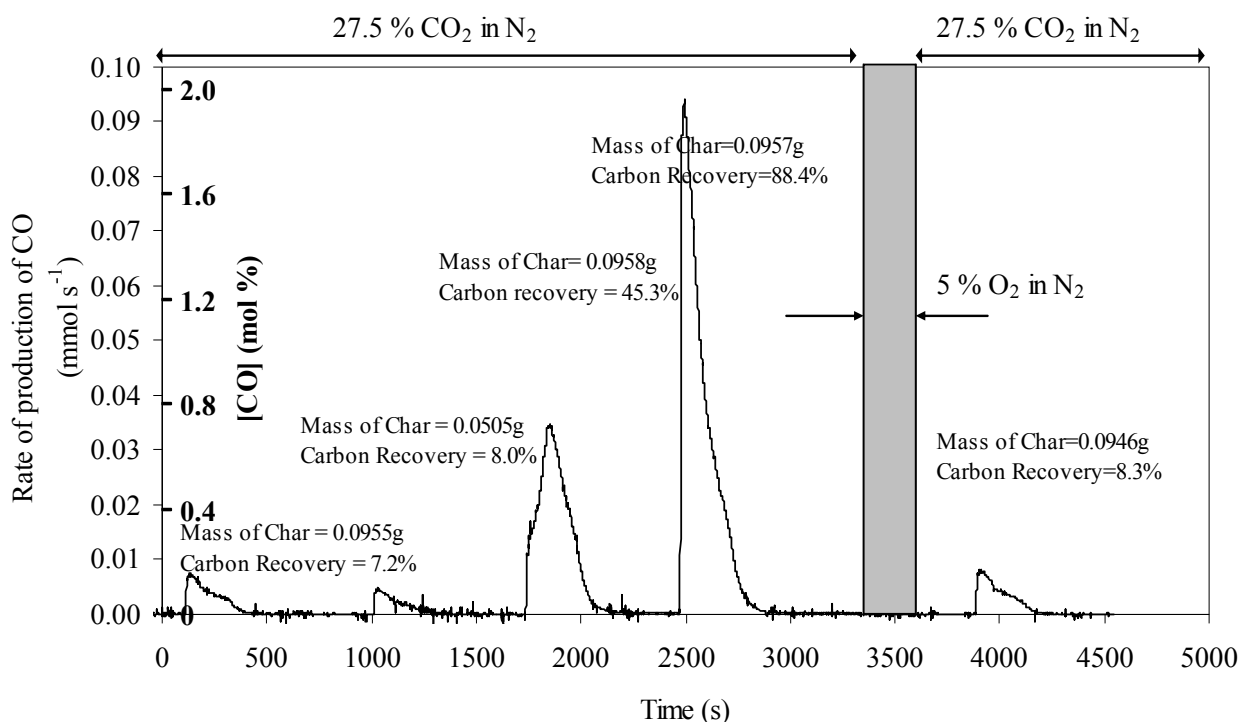


Fig. 3. A series of experiments in which successive batches of char were gasified in the active bed of Fe₂O₃ and silica sand. The bed was regenerated after the fourth batch using 5 % O₂ in N₂. In each case, the mass of char in the batch is shown, together with the recovery of carbon.

Fe₃O₄. Finally, the heights and durations of the peaks for CO in Figs. 2 and 3 indicate that gasification is probably the rate-limiting step. Consequently, the reaction of these sintered compacts of *e.g.* Fe₂O₃, appears to be sufficiently rapid at 900°C to make the above cyclic process feasible. The same experiment was also conducted with 28 mol% steam, balance N₂, as the gasifying agent [26]; in the presence of the iron oxide, even when it is spent as an oxygen carrier, the initial ratio of CO to CO₂ is smaller than when iron is not present and the gasification is carried out in a bed of pure sand. This indicates that the iron oxide is promoting the shift reaction (15). There is evidence to suggest that the overall rate of gasification is increased in the presence of the oxygen carrier [24]; however, the story is complicated and is not purely a function of the removal of inhibitory products of gasification, such as H₂ and CO: our results suggest that the volatiles content of the fuel also exerts a profound influence [41].

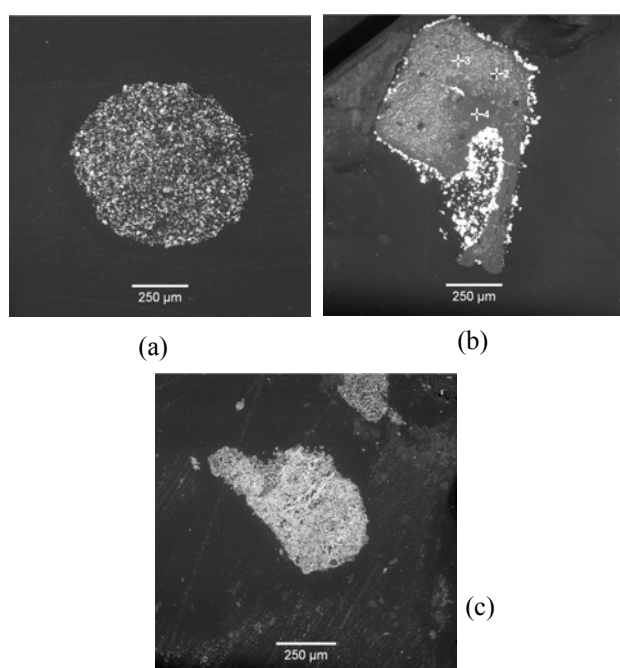


Fig. 4. Cross-sectional SEM images of unreacted carrier particles: (a) mechanically mixed, 82.5 wt% CuO, (b) wet-impregnated carrier, 78 wt% CuO, (c) co-precipitated carrier, 82.5 wt% CuO

Development and Performance of Cu-based Oxygen-carriers

Manufacture. Further work at Cambridge has focused on the development and performance of a suitable Cu-based oxygen-carrier for burning solid fuels using CLC [31]. Samples of carriers have been made from CuO and Al₂O₃ (as a support) in three different ways: mechanical mixing, wet-impregnation and co-precipitation. The details of preparation are described in detail by Chuang *et al.* [31]. The reactivity of these solids was assessed by measuring their ability to oxidise CO, when in a hot bed

of sand fluidised by a mixture of CO and N₂ in apparatus similar to that shown in Fig. 1. After that, the Cu in the carrier was oxidised back to CuO by fluidising the hot bed with air. These oxygen-carriers were tested over many such cycles of reduction and oxidation. Our work indicates that supporting CuO on Al₂O₃ enhances the ability of the resulting particles to withstand mechanical and thermal stresses in a fluidised bed. However, only co-precipitation produces particles which have a high loading of copper and do not agglomerate at 800 – 900°C. Figure 4 shows cross-sectional views of unreacted particles, manufactured by the various methods and with different loadings of CuO. Analyses of the various points on the wet-impregnated carrier, using energy dispersion by X-ray spectrometry, indicated that the bright white and grey regions in Fig. 4 correspond to CuO and Al₂O₃, respectively. In the carriers produced by mixing powders, as in Fig.4(a), the CuO and Al₂O₃ powders are fairly segregated, as represented by the distinct bright and grey areas. For the wet-impregnated carriers in Fig. 4(b), the CuO tended to concentrate at the exterior of a particle; furthermore this surface accumulation of CuO increased with the content of CuO. Neither a high degree of segregation nor a high surface concentration of CuO was observed in the co-precipitated carriers, which were much more homogenous mixtures of Al₂O₃ and CuO, as seen Fig. 4(c). It was concluded that intimate mixing of the two components at a nanometre scale is essential in avoiding agglomeration at high temperatures of operation.

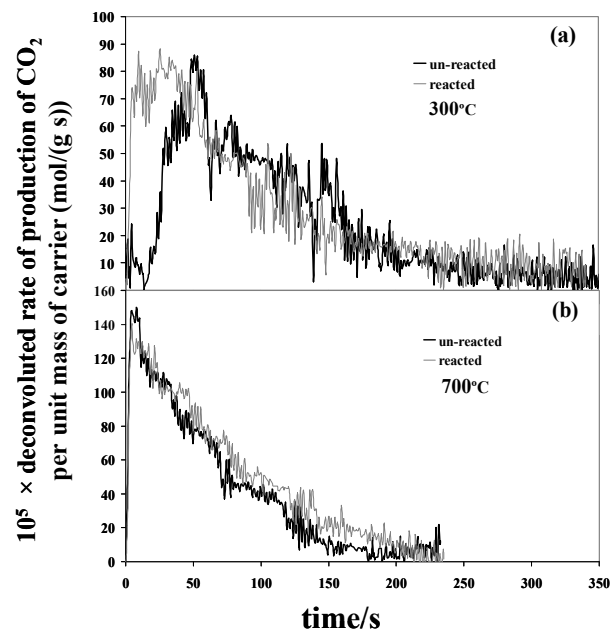


Fig. 5. Rates of production of CO₂ from CuO carrier (850-1000 μm) with 1.3 vol.% CO in N₂ at (a) 300°C and (b) 700°C. The plots refer to new oxygen-carrier or that after 5 cycles of oxidation and reduction.

Reaction Kinetics. Using apparatus similar to that shown in Fig. 1, the rates of oxidation of CO to CO₂ [42] and H₂ to H₂O [43] by particles of the co-precipitated mixture of CuO and Al₂O₃ (sieved to 355 –

500 μm), containing 82.5 wt% CuO and 17.5 wt% Al₂O₃ have been measured in a fluidised bed using, typically, either 10 mol% CO in N₂ or 10 mol% H₂ in N₂. The rates of reaction were found to be rapid, so that conditions were controlled to ensure that the measurements were not affected by interphase mass transfer between the bubble and the particulate phase of the fluidised bed reactor. The deposition of carbon by the Boudouard reaction can be a problem with CO, but was not seen in our [42] experiments. In a typical experiment, a bed of clean sand was fluidised at a given temperature between 250°C and 900°C with the mixture of CO and N₂. A known mass of the carrier was then rapidly deposited into the bed and the concentration of the off-gases as a function of time was measured. Because of the rapidity of the reaction, the off-gas trace has to be adjusted for the mixing time constant in the sampling line and analyser and this is a significant problem with this highly reactive carrier.

These techniques enabled rates of reaction to be measured from 250 to 900°C, *e.g.* as seen in Fig. 5. Using the initial rates from plots such as in Fig. 5, it was found that the order of reaction in CO was always close to unity. It was established that above 500°C, the oxidation of CO by particles of CuO of at least the size of interest in chemical looping was controlled mainly by external mass transfer. At $\sim 250^\circ\text{C}$, it appears that CO reacts directly with solid CuO in: $\text{CuO} + \text{CO} \rightarrow \text{Cu} + \text{CO}_2$, with an activation energy of 28 (± 12) kJ/mol. However, above $\sim 700^\circ\text{C}$, CuO particles seem to react by the shrinking core mechanism, predominantly involving the two consecutive reactions (8) and (9) in Table 2. The best estimate of the rate constant for reaction (9) was $9.6 \times 10^7 \exp(-56 \text{ kJ mol}^{-1}/\text{RT}) \text{ s}^{-1}$, with the activation energy correct to 12 kJ mol⁻¹; that for reaction (8) could not be measured because of its rapidity compared with reaction (9).

The kinetics of oxidation of H₂ by co-precipitated mixtures of copper oxides and Al₂O₃ are also fast at high temperatures. A combination of different particle sizes and operating temperatures had to be used [43] to minimise the impact of external mass transfer, as well as mixing in the sampling system, so that reliable measurements of rates of reaction could be made. At high temperatures ($\sim 800^\circ\text{C}$), the reaction between H₂ and CuO followed the shrinking core mechanism and proceeded *via* the intermediate, Cu₂O. The rate constants of the two consecutive reduction steps, reactions (10) and (11) in Table 2, were found to be, respectively, $6.4 \times 10^7 \exp(-58 \pm 15 \text{ kJ mol}^{-1}/\text{RT}) \text{ s}^{-1}$ and $2.1 \times 10^6 \exp(-44 \pm 10 \text{ kJ mol}^{-1}/\text{RT}) \text{ s}^{-1}$. The kinetics in the first and subsequent cycles were found to be approximately the same. At low temperatures ($\sim 300^\circ\text{C}$), the reaction in the first cycle was probably controlled to a considerable extent by nucleation initially, but the carrier reduced directly to Cu. Oxidation of Cu₂O to CuO at this temperature was slow and hence the reduced carrier could only be partially oxidised to carrier containing Cu₂O, which has a different reactivity from the carrier containing CuO.

As with reduction, the initial rates of oxidation of the co-precipitated mixture of Cu and Al₂O₃ are fast enough to be controlled largely by external mass transfer [44]. Reliable measurements of the initial rates of reaction could not be obtained above 600°C and high concentrations of O₂ (5 vol.% O₂ in N₂), owing to the reaction being too fast to follow. Nevertheless, measurements at low [O₂] have been used [44] to derive initial kinetics, after accounting for external mass transfer; in all cases, the reaction is approximately first order in oxygen concentration, for [O₂] < 0.6 mol/m³. The oxidation of carrier fully reduced to Cu apparently proceeds *via* the intermediate, Cu₂O, from 300 to 750°C and *via* a shrinking core mechanism at 800°C. For Cu₂O + 1/2O₂ \rightarrow 2CuO (reaction (13), Table 2), the rate constant was determined as $3.6 \times 10^6 \exp(-40 \pm 15 \text{ kJ mol}^{-1}/\text{RT}) \text{ s}^{-1}$, whereas for 2Cu + 1/2O₂ \rightarrow Cu₂O (reaction (12), Table 2), it is $2.3 \times 10^7 \exp(-60 \pm 15 \text{ kJ mol}^{-1}/\text{RT}) \text{ s}^{-1}$. The kinetics in later cycles of CLC can be approximated by those in the first.

Experiments with Solid Fuels

For solid fuels, the apparatus in Fig. 1 was also used [45], in which the fluidised bed was maintained at 1123 K. The bed material consisted of 20 ml sand (355 – 500 μm) and ~ 1.0 g of the co-precipitated oxygen carrier, containing CuO and Al₂O₃ (CuO:Al₂O₃ = 82.5 : 17.5 wt. %, sieved to 355 – 500 μm). Four fuels were investigated: (i) Hambach lignite (69.9 wt% C, 5.5 wt% H, 0.31 wt% S, 23.5 wt% O, and 0.94wt% N), (ii) Taldinsky bituminous coal (66.6wt% C, 5.2 wt% H, 0.30 wt% S, 27 wt% O, and 0.90 wt% N), (iii) Petroleum coke (89.9 wt% C, 3.4 wt% H, 1.08 wt% S, 4.2 wt% O, and 1.4 wt% N), and (iv) softwood chips, (46.5 wt% C, 6.1 wt% H, trace wt% S, and trace wt% N).

In an experiment, batches of solid fuel were added until the carrier was depleted. The bed was then re-oxidised and the addition continued, in a similar fashion to the feasibility studies described at the start of this section. At the commencement of each cycle, prior to the addition of solid fuels, the conversion of the CuO to Cu was tested by reacting it with cylinder synthesis gas with ratio of mol fractions CO:N₂=2:98. This procedure is referred to as a ‘titration’ in the following. The CuO was then regenerated in 5 mol % O₂ in N₂ after which the bed was fluidised with CO₂:N₂ = 23:73 mol % and batches of solid fuel (0.05 g for lignite and wood and 0.2 g for the bituminous coal and petcoke) were added to the bed until the carrier appeared to be fully depleted, *viz.* all the CuO was reduced to metallic Cu. This was assumed to occur when the addition of a batch of fuel gave the same CO concentration profile for two consecutive batches, so that only gasification was occurring in the reactor. This was confirmed by a second titration prior to regeneration to check if there was any remaining active CuO in the bed. The oxygen carrier was then re-oxidised. Here, batches of solid fuel were used to avoid the build-up of a large inventory of char.

Figure 6 shows the stability of the co-precipitated Cu-Al oxygen carrier, studied over 5 cycles; for the lignite, bituminous coal and petcoke the cyclic stability is good. However, with wood, agglomeration of the bed material occurred from cycle 3, onwards, eventually giving deactivation of the carrier. Figure 6 indicates that merging the gasification and reduction step of the oxygen carrier into one single reactor is feasible with most fuels, as the presence of ash and fines of carbon does not significantly decrease the CO₂ yield of the co-precipitated CuO-Al₂O₃. However, great care has to be taken with wood owing to the fusibility of its ash. One can also tentatively conclude that the presence of sulphur in the fuel has very little effect on the reactivity.

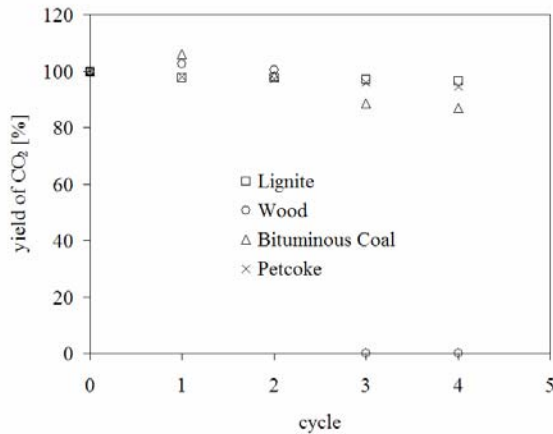


Fig. 6. Yield of CO₂ at 1123 K using a Cu-Al (CuO:Al₂O₃ = 82.5:17.5 wt.%) oxygen carrier. Batches of solid fuel were added to the bed containing the oxygen carrier.

5. THE PRODUCTION OF HYDROGEN

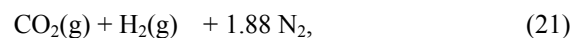
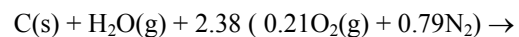
For use in current fuel cells, hydrogen must be substantially free of carbon oxides (typically < 50 ppm). We are investigating extensions of the looping method for the production of hydrogen from biomass, in a clean form suitable for direct use in a fuel cell without substantial gas clean-up, and with the production of a pure stream of CO₂ [46,47]. It is a technique primarily for use with distributed generation, suitable for local sources of biomass or waste, but potentially could lend itself to larger power stations. In our proposed process [46], the following stages are involved:

- 1) A solid fuel is gasified in steam and CO₂ to yield a syngas mostly CO and H₂, together with some CO₂, some higher hydrocarbons, including tarry substances, and H₂O.
- 2) The syngas from stage 1) is converted to a pure stream of CO₂ and steam, by passing it (in plug flow) through a packed bed of Fe₂O₃. In this bed, three oxides of Fe are involved in reactions (15) to (18) in Table 2, so that the Fe₂O₃ is finally reduced to Fe_{0.947}O. At 900°C, thermodynamic calculations show that reactions (15) and (17) are favoured when $P_{CO}/P_{CO_2} > 1.5 \times 10^{-5}$ and $P_{H_2}/P_{H_2O} > 1.2 \times 10^{-5}$, so both reactions (15) and (17) lie essentially

well to the right when reducing gases are present. Thus in the packed bed, provided it is sufficiently long, there will be a region of Fe₂O₃ at the outlet, preceded by a region of Fe₃O₄. At the entrance to the bed, [CO] and [H₂] are high. This means that the Fe₃O₄ first formed there by reactions (15) and (17) can react further by reactions (16) and (18). Thus, at 900 °C, for the Fe₃O₄ to be reduced to Fe_{0.947}O, $P_{CO}/P_{CO_2} > 0.49$, which will be the case if there is significant conversion of CO₂ to CO in the gasifier. Similarly, for the Fe₃O₄ to be reduced to Fe_{0.947}O by hydrogen would require $P_{H_2}/P_{H_2O} > 0.39$; this is likely for a typical syngas. Accordingly, at the entrance to the bed will be a region of Fe_{0.947}O. As time proceeds, there will, in effect be two fronts moving through the bed: one defines the boundary between Fe_{0.947}O and Fe₃O₄ and the other, nearer the exit, forms the boundary between Fe₃O₄ and Fe₂O₃. The flow of syngas to the packed bed would be stopped just before the Fe₃O₄ / Fe₂O₃ front breaks through the bed, to avoid any slip of CO into the outlet stream of gas. Accordingly, the outlet from this bed would be a stream of pure CO₂ and some water, which could be condensed out, allowing sequestration of the CO₂ if required. A proportion of the CO₂ would be recycled to the gasifier. One advantage of using iron oxide is that it catalyses the decomposition of tars, giving a clean off-gas and also a bed free from tarry deposits.

- 3) Production of hydrogen. Hydrogen would be generated from the spent bed in 2) by passing steam through it, thus reversing reaction (18) in Table 2. For this to be the case, $P_{H_2}/P_{H_2O} < 0.39$, so the hydrogen would occur with a front of Fe₃O₄ propagating from the entrance until it reaches the Fe₃O₄ left at the end of stage 2).
- 4) Regeneration of Fe₂O₃. Once the bed has been sufficiently converted in 3), air is supplied to the bed to oxidise the Fe₃O₄ to Fe₂O₃; the products being depleted air and energy. The hot, depleted air leaves the oxidation reactor at high temperature (*ca.* 1000°C) and so can be used to raise steam or, when the operation is pressurised, to drive a gas turbine topping cycle. Our research [46] shows this to be a rapid reaction.
- 5) Finally, the cycle is repeated, with the supply of syngas recommenced to the bed regenerated in 4). A cyclic operation can be arranged, enabling the gasifier to operate continuously.

The overall reaction, assuming that gasification of pure carbon were being undertaken, is:



which has a net enthalpy $\Delta H^0 = -151$ kJ/mol. Hence, by suitable heat integration of the operations, it would be possible to run the process, produce pure streams of CO₂ and H₂ and to export some heat. Importantly, each

of the products in Reaction (21) would be in a separate stream. Thermochemical calculations for the individual stages shows gasification reaction (7), at 900°C, to have $\Delta H_{1173K}^0 = +169$ kJ/mol, stage 3) to have $\Delta H_{1173K}^0 = -43$ kJ/mol and stage 4) $\Delta H_{1173K}^0 = +168.9$ kJ/mol -122 kJ/mol of Fe₃O₄ oxidised. Stage 2) depends on the syngas composition: if gasification were by CO₂ only, it would be slightly exothermic, overall, becoming more endothermic as the proportion of hydrogen increases. The **process engineering** of this to a practicable scheme represents a very significant challenge because of the need to integrate the flows of enthalpy. One approach is to immerse a number of packed bed reactors, containing the iron oxide particles, within a fluidised bed gasifier, allowing the excellent heat transfer provided by the fluidisation to enable ready transfer of heat between the enthalpy-producing and enthalpy-requiring stages, with the packed bed reactors manifolded so that they can execute the various sequences of operation. The complexity of the challenge is balanced by the advantages of the proposed process, which includes the fact that the conveying of hot metal oxide between fuel and air reactors, used in conventional CLC, is avoided.

Results

Simulated Synthesis Gases. Initial research has mainly focused on the use of fairly pure gaseous fuels, *e.g.* cylinder gas mixtures to “simulate” the syngas leaving a typical gasifier [46]. Typical apparatus used to study the reactions is shown in Fig. 7, which can be maintained at a fixed temperature by insertion into an electrically-heated furnace.

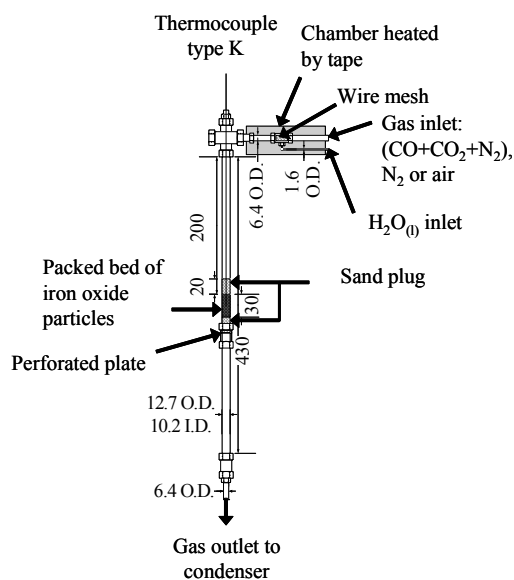


Fig. 7. Laboratory-scale packed bed reactor for experiments with iron oxides, using simulated gases flowing at 1 – 2 l/min (at STP) [46].

Initial results are promising: Fig. 8 shows one cycle performed in a bed such that the ratio of partial pressures of CO to CO₂ was sufficient to prevent

reduction of the oxide completely to metallic iron. The results indicate that very pure hydrogen can be produced, whilst the iron oxide, produced as described in section 4, above, maintains its activity over many cycles. Results also show that, although it might be desirable from point of view of oxygen carrying capacity to reduce the oxide to metal, doing so with pure oxides results in sintering and deactivation of the bed after only a few cycles. The Boudouard reaction only becomes significant below 600°C and so can be avoided in these experiments [46].

Cleaton *et al.* [48] have experimented with co-precipitated particles involving the oxides of aluminium and iron in which Al was added such that the ratio of Fe:Al by weight was 9:1. It was shown that co-precipitated particles might be able to achieve consistently high H₂ yields when cycling between Fe₃O₄ and Fe, and that these yields are a function of the ratio of [CO₂] to [CO] during reduction, where thermodynamic arguments suggest that the yield should be independent of this ratio. A striking feature with these materials was that particles made by mechanical mixing performed much better than those made by co-precipitation when cycling between Fe₃O₄ and Fe_{0.947}O, but much worse than co-precipitated particles when cycling between Fe₃O₄ and Fe.

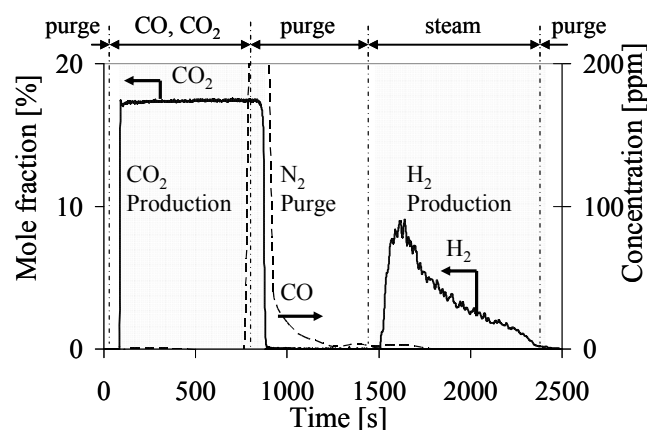


Fig. 8. Reduction and subsequent oxidation in steam for the transition from Fe₂O₃ to Fe_{0.947}O at 1023 K with a 20 g charge of Fe₂O₃ in the apparatus of Fig. 7. The dashed vertical lines (---) indicate the times when the inlet gas to the reactor was changed. Flowrates/compositions: purge – 0.12 m³/h, 100% N₂; CO,CO₂ - 0.12 m³/h; 8.9 % CO, 8.6% CO₂, balance N₂; steam – 1.5 × 10⁻⁵ m³/h H₂O(l), 0.06 m³/h N₂ (~ 25 % steam in N₂).

Experiments with Gasifier Gases. Further experiments have been undertaken on the reactivity of this system using actual gasifier gases [45]. In the fluidised bed gasifier, char made from lignite (Sigma Aldrich, 75.9 wt% C, 1.0 wt% H, trace wt% S, 6.0 wt% O and 0.73 wt% N) was gasified by air and the resulting syngas was directed through a packed bed containing iron oxide,

constructed as in Fig. 7. The iron oxide particles were prepared *via* the mechanical mixing technique, described in Section 4, from Fe_2O_3 powder ($< 5 \mu\text{m}$, Sigma-Aldrich, $> 99 \text{ wt}\%$). A typical experiment was performed by allowing the gasifier to reach a steady state outlet concentration of $[\text{CO}]$ and $[\text{CO}_2]$, while purging the packed bed with nitrogen. Next, the off-gas from the gasifier was diverted through the packed bed until the outlet composition of the gases was equal to that entering from the gasifier. The packed bed was subsequently purged with N_2 for 500 s. The reduced iron was then re-oxidized to Fe_3O_4 by a mixture of steam and N_2 ($[\text{H}_2\text{O}]:[\text{N}_2] = 20:80 \text{ mol}\%$) for 1700 s.

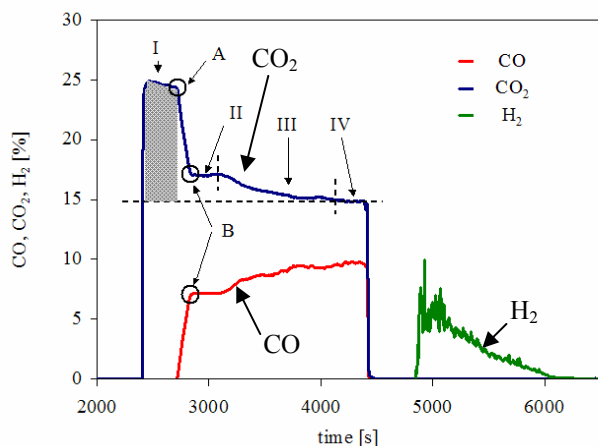


Fig. 9. Reduction and subsequent oxidation in steam for the transition from Fe_2O_3 to $\text{Fe}_{0.947}\text{O}$ at 1083 K in a bed of 20 g Fe_2O_3 , using gasifier gas.

Figure 9 shows the composition of the effluent gas as a function of time for a bed containing 20 g of Fe_2O_3 , operated at 1083 K. Initially, all of the syngas (flow-rate 2.1 L/min at STP) entering the bed was converted into CO_2 . This period is labelled (I) and lasted for ~ 300 s. A simple mass balance on the CO_2 produced during the time of zero CO slip (grey shaded area) shows that all the Fe_2O_3 is converted to Fe_3O_4 . In addition only a minimal amount of the Fe_3O_4 is further reduced to $\text{Fe}_{0.947}\text{O}$ during this time ($\sim 3 \text{ mol}\%$). Thus, the kinetics for the Fe_2O_3 - Fe_3O_4 transition are fast enough to reach equilibrium within the residence time of the gas in the bed, which for the given conditions was ~ 0.19 s. After the breakthrough of CO (point A in Fig. 9), *i.e.* the point at which all the Fe_2O_3 has been converted to Fe_3O_4 or $\text{Fe}_{0.947}\text{O}$ in the reactor (based on a mass balance on the exit CO_2 stream), the Fe_3O_4 - $\text{Fe}_{0.947}\text{O}$ equilibrium transition is reached. For the transition from Fe_3O_4 to $\text{Fe}_{0.947}\text{O}$ thermodynamics gives $K_p = P_{\text{CO}_2}/P_{\text{CO}} = 2.27$ at 1083 K. This equilibrium value corresponds to the kink in Fig. 9, at point B. The experimentally-calculated $K_p = 2.37$, and is thus very close to the theoretical value. After the kink, a region of flat $[\text{CO}_2]$ and $[\text{CO}]$ profiles can be observed, labelled II. This period lasted ~ 240 s, during which the kinetics of the Fe_3O_4 - $\text{Fe}_{0.947}\text{O}$ transition are fast enough to reach equilibrium within the residence time of the reactor. However, as the reaction rates decrease with conversion, starting from $t = 3130$ s the kinetics were not sufficiently rapid to reach

equilibrium within the residence time of the gas in the bed. This yielded a period, labelled III, of continuously-decreasing $[\text{CO}_2]$ and increasing $[\text{CO}]$ in the effluent gas. Given that, after that point, a constant ratio of mole fraction of CO to that of CO_2 can be observed, it is assumed that all the Fe_3O_4 which can be converted has been converted to $\text{Fe}_{0.947}\text{O}$, and the syngas at the gasifier concentration breaks through. This period is labelled IV. It can be seen from Fig. 9 that the composition of the syngas leaving the gasifier is $[\text{CO}_2]:[\text{CO}] \approx 15:10$ (on a N_2 -free, molar basis).

After the breakthrough of the syngas, the gasifier gas was disconnected and the bed was subsequently purged for 500 s with N_2 (flow-rate 2 L/min at STP). Starting from $t = 4850$ s, the reduced iron oxide was re-oxidised by a stream of gas containing $[\text{H}_2\text{O}]:[\text{N}_2] = 20:80 \text{ mol}\%$ (flowrate of $\text{N}_2 = 2 \text{ L/min}$ at STP) stream to Fe_3O_4 . A mass balance reveals, that, assuming all Fe_2O_3 is converted to Fe_3O_4 , 70 mol % of the Fe_3O_4 was further reduced to $\text{Fe}_{0.947}\text{O}$ during the reduction period. Bohn *et al.*⁴⁶ reported conversion rates of $\sim 80 - 85\%$ for the Fe_2O_3 - $\text{Fe}_{0.947}\text{O}$ transition if a syngas mixture from cylinders is used. This would imply that using the syngas from an actual gasifier, slightly smaller conversion rates can be expected, at least in the case of lignite char. Further studies are investigating the stability in extended cycles and with different fuels, *e.g.* high-rank coals, biomass *etc.*

6. CONCLUSIONS

There is little doubt that chemical looping combustion for the combustion of natural gas, or clean synthesis gas, could be brought to the industrial scale readily [1,14]. Extended testing of carrier particles is still needed at the large scale, but there has been sufficient research activity to enable scale-up with some confidence. However, further research on the important topic of solid fuels is needed. To date, three broad options have evolved to cope with solid fuels:

- (i) Gasify the solid fuel separately and burn the synthesis gas using a conventional chemical CLC arrangement for gaseous fuels.
- (ii) Gasify the solid fuel *in situ* in the presence of a batch of metal oxide in a single reactor. There is no throughflow of solids: when the metal oxide is depleted, the feed of fuel is discontinued and the contents are re-oxidised by the admission of air to the reactor, once the fuel inventory has been reduced sufficiently by gasification.
- (iii) Gasify the solid fuel *in situ* in the presence of the metal oxide in a fuel reactor: separate the unburnt fuel from the spent oxide before the carrier solids are passed to the oxidation reactor.

In each case, the gasifying agent would need to be free from nitrogen, *e.g.* pure steam, pure CO_2 , or mixtures thereof. Option (ii) has the advantage that the conveying of solids external to the reactor is eliminated, with concomitant reduction in the rate of attrition of looping particles caused by circulation. However, the choice of oxides is rather restricted because it requires

an oxide which is exothermic during reduction to balance the endothermic gasification reactions. Copper has such oxides, but temperatures must be limited to < 900°C to avoid sintering and deactivation of the carrier in its reduced form. Option (iii) has, to date, been the only technique tested at reasonable scale, with relatively good results. One advantage of (iii) is that relatively cheap materials (*e.g.* natural ilmenite) can be used, since the enthalpy is balanced by the recirculation of particles from the oxidation reactor, thereby removing the need to use one of the few oxides which undergo both exothermic reduction and exothermic oxidation reactions. On the negative side is the potential for increased attrition caused by the conveying and recycling of solids. As Option (i) also requires that the gasifier be gasified solely by CO₂, steam or mixtures thereof, the problem arises as to how to balance the endothermic gasification reactions.

One problem with all of the options is the potential for the build-up of an inventory of unreactive char. This, of course, depends on the type of fuel and there is *some* evidence that gasification rates are faster in the presence of looping agent; however, the reasons for this are unclear: it might be dependent on the type of fuel used, particularly its content of volatile matter. Further studies are needed. Agglomeration of the carrier in options (ii) and (iii) is a particular problem if a woody feedstock is used, especially under reducing conditions, in which the ash is fusible.

Hydrogen is, currently, the most desirable fuel for use in the present generation of practicable solid oxide fuel cells. A modification of chemical looping, using the oxides of iron, offers substantial benefits. In fact, it might be a low cost option for the initial industrial realisation of the looping technique. However, the detailed engineering requires further work to test the integration of the heat loads, control of the overall operation, and the longevity of the carrier particles.

In summary, the chemical looping of solid fuels has been demonstrated, at the small scale, to be feasible. However, extended running in much larger systems to evaluate the performance of different combinations of carriers and fuels is at scale and over many hundreds of cycles is now required. Thus, it is timely for there to be a major European initiative to work on the scale-up and industrial demonstration of the technique, given the high level of expertise in chemical looping in a number of institutions in Europe.

Acknowledgements

The author is grateful to the Engineering and Physical Sciences and Research Council (EPSRC) for financial support.

References

[1] E.J. Anthony, *Ind. Eng. Chem. Res.* 47 (2008) 1747-1754.
 [2] Q. Song, R. Xiao, Z. Deng, L. Shen, J. Xiao & M. Zhang, *Ind. Eng. Chem. Res.* 47 (2008) 8148-8159.
 [3] S.A. Scott, J.S. Dennis, A.N. Hayhurst & T. Brown, *AIChE J.* 52 (2006) 3325-3328.
 [4] H. Leion, T. Mattisson & A. Lyngfelt, *Fuel* 86 (2007) 1947-1958.

[5] IPCC (2001). *Climate Change 2001*. Third Assessment Report, Intergovernmental Panel on Climate Change (IPCC), U.N.
 [6] International Energy Agency (2006). *World Energy Outlook*, OECD IEA, Paris.
 [7] A. Lyngfelt, B. Leckner & T. Mattisson, *Chem. Eng. Sci.* 56 (2001) 3101-3113.
 [8] J. Davison, *Energy* 32 (2007) 1163-1176.
 [9] B. Kronberger, A. Lyngfelt, G. Löffler & H. Hofbauer, *Ind. Eng. Chem. Res.* 44 (2005) 546-556.
 [10] J. Ishida, H. Jin & T. Okamoto, *Energy Fuels* 12 (1998) 223-229.
 [11] T. Mattisson, A. Lyngfelt & P. Cho, *Fuel* 80 (2001) 1953-1962.
 [12] L.F. de Diego, F. Garcia-Labiano, J. Adanez, P. Gayan, B.M. Corbella & J.M. Palacios, *Fuel* 83 (2004) 1749-1757.
 [13] B.M. Corbella, L. de Diego, F. Garcia, J. Adanez & J.M. Palacios, *Energy Fuels* 19 (2005) 433-441.
 [14] A. Lyngfelt, B. Kronberger, J. Adanez, J.-X. Morin & P. Hurst (2004). The Grace Project Development of Oxygen Carrier particles for Chemical Looping Combustion. Design and Operation of a 10 kW Chemical Looping Combustor. Presented at the *Seventh Int. Conf. on Greenhouse Gas Control*, Vancouver, Canada.
 [15] L.F. de Diego, F. Garcia-Labiano, P. Gayan, J. Celaya, J.M. Palacios & J. Adanez, *Fuel* 86 (2007) 1036-1045.
 [16] M. Ishida, D. Zheng & T. Akehata, *Energy* 12 (1987) 147-154.
 [17] J. Wolf, M. Anhedén & J. Yan, *Fuel* 84 (2005) 993-1006.
 [18] H.M. Kvamsdal, K. Jordal & O. Bolland, *Energy* 32 (2007) 10-24.
 [19] N.R. McGlashan, *Proc. I.Mech.E. Part C* 222 (2008) 1005-1019.
 [20] M. Ishida & H. Jin, *J. Chem. Eng. Japan* 27 (1994) 296-302.
 [21] J. Adánez, P. Gayán, J. Celaya, L.F. de Diego, F. García-Labiano & A. Abad, *Ind. Eng. Chem. Res.* 45 (2006) 6075-6080.
 [22] B.J. McBride, M.J. Zehe & S. Gordon (2002). NASA Glenn Coefficients for Calculating Thermodynamic Properties of Individual Species. NASA. 2002 report TP-2002-21155.
 [23] K.G. Denbigh, *Chem. Eng. Sci.* 1 (1956) 1-9.
 [24] H. Leion, T. Mattisson & A. Lyngfelt, *Int. J. Greenhouse Gas Control* 2 (2008) 180-193.
 [25] R.K. Lyon & J.A. Cole, *Comb. Flame* 121 (2000) 249-261.
 [26] J.S. Dennis, S.A. Scott & A.N. Hayhurst, *J. Energy Institute* 79 (2006) 187-190.
 [27] N. Berguerand & A. Lyngfelt, *Fuel* 87 (2008) 2713-2726.
 [28] A. Abad, T. Mattisson, A. Lyngfelt & M. Johansson, *Fuel* 86 (2007) 1021-1035.
 [29] Y. Cao & W.P. Pan, *Energy Fuels* 20 (2006) 1836-1844.
 [30] A. Abad, F. Garcia-Labiano, L.F. de Diego, P. Gayan & J. Adanez, *Energy Fuels* 21 (2007) 1843-1850.
 [31] S.Y. Chuang, J.S. Dennis, A.N. Hayhurst, A.N. & S.A. Scott, *Comb. Flame* 154 (2008) 109-121.
 [32] M.M. Hosain & H.I. de Lasa, *Chem. Eng. Sci.* 63 (2008) 4433-4451.
 [33] Q. Song, R. Xiao, Z. Deng, W. Zheng, L. Shen & J. Xiao, *Energy Fuels* 22 (2008) 3661-3672.
 [34] T. Mattisson, A. Jardnas & A. Lyngfelt, *Energy & Fuels* 17 (2003) 643 - 651.
 [35] P. Cho, T. Mattisson. & A. Lyngfelt, *Fuel* 83 (2004) 1215-1225.

- [36] B. Corbella, L.F. de Diego, F. García-Labiano, J. Adánez & J. Palacios, *Ind. Eng. Chem. Res.* 45 (2004) 157-165.
- [37] S.R. Son & S.D. Kim, *Ind. Eng. Chem. Res.* 45 (2006) 2689-2696.
- [38] P. Cho, T. Mattisson & A. Lyngfelt, *Ind. Eng. Chem. Res.* 44 (2005) 668-676.
- [39] Q. Zafar, T. Mattisson & B. Gevert, *Energy & Fuels* 20 (2006) 34-44.
- [40] T. Mattisson & A. Lyngfelt, (2001). Capture of CO₂ using chemical-looping combustion. First Biennial Meeting of the Scandinavian – Nordic Section of the Combustion Institute, Göteborg, Sweden, April 18-20, 2001, p163-168.
- [41] T.A. Brown, S.A. Scott & J.S. Dennis, J.S. (2009). The effect of type of fuel on the kinetics of the chemical looping of solid fuels. Paper submitted to *Fuel*, February, 2009.
- [42] S.Y. Chuang, J.S. Dennis, A.N. Hayhurst & S.A. Scott, *Proc. Combustion Institute* 32 (2009) 2633-2640.
- [43] S.Y. Chuang, J.S. Dennis, A.N. Hayhurst & S.A. Scott (2009). Kinetics of the chemical looping oxidation of H₂ by a co-precipitated mixture of CuO and Al₂O₃. Paper submitted to *Fuel*, January, 2009.
- [44] S.Y. Chuang, J.S. Dennis, A.N. Hayhurst & S.A. Scott (2009). Kinetics of the chemical-looping oxidation of a co-precipitated mixture of Cu and Al₂O₃ by O₂. Paper submitted to *FBC 20*, December, 2008.
- [45] C.R. Mueller, T.A. Brown, C.D. Bohn, S.Y. Chuang, J.P.E. Cleeton, S.A. Scott & J.S. Dennis (2009). Experimental investigation of two modified chemical looping combustion cycles using syngas from cylinders and the gasification of solid fuels. Paper submitted to *FBC 20*, December, 2008.
- [46] C.D. Bohn, C. Mueller, J.P.E. Cleeton, A.N. Hayhurst, J.F. Davidson, S.A. Scott & J.S. Dennis, *Ind. Eng. Chem. Res.* 47 (2008) 7623-7630.
- [47] J.P.E. Cleeton, C.D. Bohn, C.R. Müller, J.S. Dennis & S.A. Scott, *Int. J. Hydrogen Energy* (2008) in press.
- [48] J.P.E. Cleeton, C.D. Bohn, C.R. Müller, J.S. Dennis & S.A. Scott (2009). Different methods of manufacturing Fe-based oxygen carrier particles for chemical looping combustion, and their effect on performance. Paper submitted to *FBC 20*, December, 2008.